Water Resources Research

RESEARCH ARTICLE
10.1029/2022WR032712

Drought Conditions Enhance Groundwater Table Fluctuations Caused by Hydropower Plant Management

M. Basilio Hazas[1], G. Marcolini[2], M. Castagna[1], M. Galli[1], T. Singh[2], B. Wohlmuth[2], and G. Chiogna[1]

[1]School of Engineering and Design, Technical University of Munich, Munich, Germany, [2]Department of Numerical Mathematics, Technical University of Munich, Garching, Germany

Key Points:

- Wavelet power spectrum and coherence analysis is used to study river-aquifer interactions under dam operations in an Alpine catchment
- The impact of reservoir operations on the aquifer is strongest under low flow conditions but the area impacted shows little variation
- Under low flow conditions, dam operations considerably influence the frequency of the water exchange between rivers and aquifer

Supporting Information:

Supporting Information may be found in the online version of this article.

Correspondence to:

G. Chiogna,
gabriele.chiogna@tum.de

Citation:

Basilio Hazas, M., Marcolini, G., Castagna, M., Galli, M., Singh, T., Wohlmuth, B., & Chiogna, G. (2022). Drought conditions enhance groundwater table fluctuations caused by hydropower plant management. *Water Resources Research*, *58*, e2022WR032712. https://doi.org/10.1029/2022WR032712

Received 2 MAY 2022
Accepted 27 SEP 2022

Abstract Management of hydropower plants strongly influences streamflow dynamics and hence the interaction between surface water and groundwater. As dam operations cause variations in river stages, these can result in changes in the groundwater level at multiple temporal scales. In this work, we study the case of an Alpine aquifer, where weekly fluctuations are particularly pronounced. We consider an area with four river reaches differently impacted by reservoir operations and investigate the influence of these rivers on the common aquifer. Using continuous wavelet transform and wavelet coherence analysis, we show that weekly fluctuations in the groundwater table are particularly pronounced in dry years, in particular in the winter season, although the area of the aquifer impacted by dam operations remains almost unchanged. We thus observe that in Alpine catchments, surface water-groundwater interaction is sensitive to the conditions determined by a specific hydrological year. We also investigate the influences of the river-aquifer water fluxes and show that under dry conditions hydropeaking mainly affects their temporal dynamics. Our observations have significant consequences for predicting nutrient and temperature dynamics/regimes in river-aquifer systems impacted by hydropower plant management.

Plain Language Summary The operation of hydropower plants affects the water level in the downstream part of the river, which in turn can alter the groundwater level. In this work, we study an Alpine aquifer crossed by rivers differently impacted by hydropower production. We use statistical tools to analyze the interaction between the rivers and the groundwater, and observe that this interaction is sensitive to the conditions of the hydrological year, such as dry periods.

1. Introduction

Montanari et al. (2015) stated that "The interaction between human and water systems needs to be analyzed from new perspectives to develop a comprehensive picture of the inherent feedbacks and coevolving processes and scenarios." One of the most prominent examples of such interaction is hydropower production and the feedback processes that it generates on the natural environment (Hauer et al., 2017), including sediment transport (Béjar et al., 2018; Hauer et al., 2019), biological process in the riverine environment (Bejarano et al., 2018; Bruno et al., 2009; Person, 2013), the hydrological cycle (Shuai et al., 2019; Yellen & Boutt, 2015), biogeochemical processes (Graham et al., 2019), energy cycle (Wu et al., 2020), and surface water — groundwater interaction (Sawyer et al., 2009; Shuai et al., 2017). For instance, hydropeaking, that is, sharp fluctuations in the river stage caused by the management of storage hydropower plants, has important consequences on flow and transport processes in rivers. Furthermore, it can also influence the aquifers even 100 km downstream from the hydropower dam (Ferencz et al., 2019) and tens of meters far from the river (Sawyer et al., 2009; Zachara et al., 2016, 2020), including riverine islands (Francis et al., 2010).

Surface water-groundwater interaction is affected by the morphological characteristics of the riverbed (Schmadel et al., 2017; Singh et al., 2019; Wu et al., 2018) and the subsurface (Shuai et al., 2019), as well as by seasonal hydrological variability. For example, hydropeaking is stronger during dry periods (Li & Pasternack, 2021) or more in general low flow conditions (Chiogna, Marcolini, et al., 2018). In this sense, Song et al. (2018) illustrated how the effect of dam operations on the aquifer system depends on drought conditions of the catchment using numerical simulations. They also showed that to describe surface water-groundwater interaction it is important to consider the complex feedback between hydrological processes and water management.

Several studies have focused on surface water-groundwater interaction under altered streamflow conditions in different regions, such as the Colorado River (Francis et al., 2010; Sawyer et al., 2009), and the Deerfield River (Boutt & Fleming, 2009; Yellen & Boutt, 2015) in the USA, the Cockburn River in Australia (McCallum & Shanafield, 2016; Welch et al., 2013), the Danube River in the Austrian part (Derx et al., 2010), and the Lundesokna River in Norway (Casas-Mulet et al., 2015), as well as synthetics models (e.g., Ferencz et al., 2019; Schmadel et al., 2016). These studies have addressed mainly the hydrological and geochemical interaction between surface water and the hyporheic zone or its proximity. At larger spatio-temporal scales, recent works in the Columbia River analyzed the effect of the river fluctuations on exchange flows and contaminant plumes along the river reach (Shuai et al., 2019) and the river corridor (Rizzo et al., 2020; Song et al., 2020; Zachara et al., 2016, 2020). Little research on surface water-groundwater interaction has been done on Alpine aquifers, with exceptions such as Fette et al. (2007) who studied the upper Rhône River. In Alpine catchments, variability with a period of 7 days is particularly relevant for hydrological studies focusing on water management because it represents the lower energy production typically occurring over weekends (Chiogna, Marcolini, et al., 2018; Majone et al., 2016; Pérez Ciria et al., 2019). Furthermore, this periodic signal can propagate in the aquifer farther than the sub-daily fluctuations (Sawyer et al., 2009; Singh, 2004).

The aim of our work is to analyze the impact of fluctuations caused by dam operations on the groundwater considering the propagation of the weekly signal and its evolution in time and to observe how this changes in two different hydrological years (i.e., a wet and a dry year). Specifically, we study the Adige Valley aquifer, which is affected by several rivers impacted by hydropower operations. This area represents a typical scenario in Alpine catchments, where multiple regulated rivers can converge in relatively narrow valleys (Pérez Ciria et al., 2019).

In this study, we develop a transient groundwater flow model to capture the aquifer's response to streamflow alterations with a weekly periodicity since observations with high spatio-temporal resolution are hardly available for large (i.e., greater than 10 km^2) aquifers. We compare two different hydrological conditions corresponding to the hydrological years 2009/10 and 2016/17. The first one represents a typical year in terms of temperature and precipitation. The latter is characterized by a drought caused by the lack of winter precipitation, which leads to low summer streamflow conditions (Chiogna, Skrobanek, et al., 2018). We introduce the use of wavelet maps to analyze the coherence between weekly signal in the rivers and the whole modeled aquifer. The variability in the environmental and hydrological conditions encountered in this case study helps to validate this methodology for its application to other scenarios.

Wavelet analysis is a powerful tool to investigate non-stationary periodicities in hydrological time series. It has been applied to study time series in different (hydro)geological systems (Lu et al., 2015; Song et al., 2020; Tenorio-Fernandez et al., 2019; Wright et al., 2015), and more recently in the context of surface water-groundwater interaction to study hyporheic exchange flows (Chen et al., 2022). In this study, we apply the continuous wavelet transform (Torrence & Compo, 1998) and the wavelet coherence analysis (Grinsted et al., 2004) for three river discharge time series of the Adige catchment with different degrees of alteration under the same climatic and geologic conditions. As most of the large scale studies on surface water-groundwater interaction focus on a single river-aquifer system (Ferencz et al., 2019; Francis et al., 2010; Song et al., 2018; Zachara et al., 2016), this is one of the first works including such complex hydrological system where multiple impacted rivers exchange water with the same aquifer.

The manuscript is organized in the following way: Section 2 describes the study area and the used data set. Section 3 introduces the modeling approach. In Section 4, we describe the continuous wavelet transform and wavelet coherence analysis, and explain how we apply them to create the wavelet maps. Section 5 shows through a wavelet transform analysis how the aquifer is affected by water management and the consequences on the surface-water groundwater flux exchange in a wet and a dry year. In Sections 6 and 7, we discuss the implication of our results and, finally present the conclusions of our research study, respectively.

2. Study Area

The study site is located within the Adige catchment, in the northeast of Italy. It covers an area of about 30 km^2, which includes the Adige aquifer in the north of Trento (Figure 1). The area is traversed by the Adige River and two important tributaries: the Noce River and the Avisio River. These rivers, in particular the Noce and the Adige, are impacted by the operation of hydropower plants. In fact, the Adige catchment provides water for

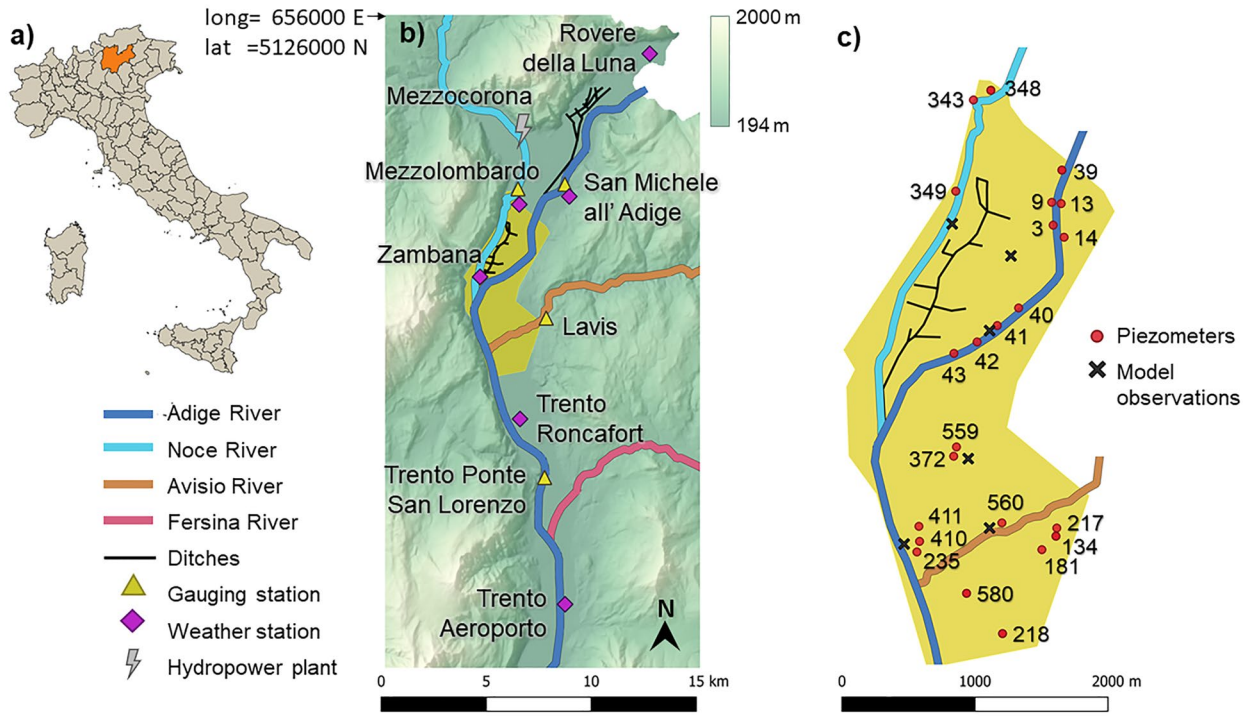

Figure 1. (a) Map of Italy with Trentino highlighted; (b) close-up to the Adige Valley with the modeled area highlighted in yellow and (c) modeled area, also depicting the locations of piezometers and model observations used in the presented study.

34 hydropower plants and approximately 1,050 small hydropower plants are distributed within the river basin (Chiogna et al., 2016). The region's climate is sub-alpine, composed of dry winters, snowmelt in spring, and humid summers leading to well-suited conditions for hydropower production in the Adige River basin (Chiogna et al., 2016; Perez Ciria et al., 2019). The long-term mean annual precipitation is 1,022 mm (Castagna et al., 2015), and the mean seasonal temperature in the valley varies between −4°C in winter and 29°C in summer.

The geology of the Adige Valley is characterized by a multilayer aquifer system of sandy-gravelly material, interconnected with sandy-silty layers in-between (Autorità di Bacino del Fiume Adige, 2007). The main shallow phreatic aquifer is a semiconfined aquifer with a maximum thickness that varies between 50 and 60 m (Autorità di bacino distrettuale delle Alpi Orientali, 2010; Viesi et al., 2016). Quaternary deposits present in the valley mainly consist of fine material, and lateral and alluvial fans from the tributaries of the Adige River, composed of sandy-gravelly material with a hydraulic conductivity between 10^{-3} m/s and 10^{-5} m/s (Autorità di bacino distrettuale delle Alpi Orientali, 2010). The aquifer is recharged by lateral springs corresponding to the Noce and Avisio Fans (Castagna et al., 2015). The shallow aquifer close to the Avisio Fan has a maximum depth of 20 m, and its depth reaches 6–7 m in areas close to the Adige River. The maximum depth of the shallow aquifer located in the Piana Rotaliana, where the Noce River flows, is about 17 m, while it reaches a very shallow depth (up to 1 m) in Nave San Rocco (Autorità di Bacino del Fiume Adige, 2007). The resulting system is very complex, with a multi-aquifer water circulation. This is mainly because the impermeable bed layers are irregular, which results in interconnections between different aquifers (Viesi et al., 2016). Also, it is important to consider that the Adige Valley is included in carbonate massifs which contribute to lateral recharges for the aquifers (Autorità di bacino distrettuale delle Alpi Orientali, 2010; Viesi et al., 2016).

Snow and glacier melting control the natural recharge of the Adige aquifer, although human activity, such as hydropower production and agriculture, also play a significant role in the aquifer dynamics (Castagna et al., 2015; Chiogna et al., 2016). The aquifer is exploited by 2070 wells spread along the whole valley, with pumping rates that vary seasonally according to agricultural needs (Beretta, 2011; Castagna et al., 2015). Moreover, five well fields extract water for the drinking water supply system of the city of Trento. The most important well field is located in the Avisio Fan, with a mean extraction rate of 208l/s (Castagna et al., 2015). Finally, since the area used to be a wetland, a network of ditches (Figure 1c) is present in the reclaimed zones. The water into the

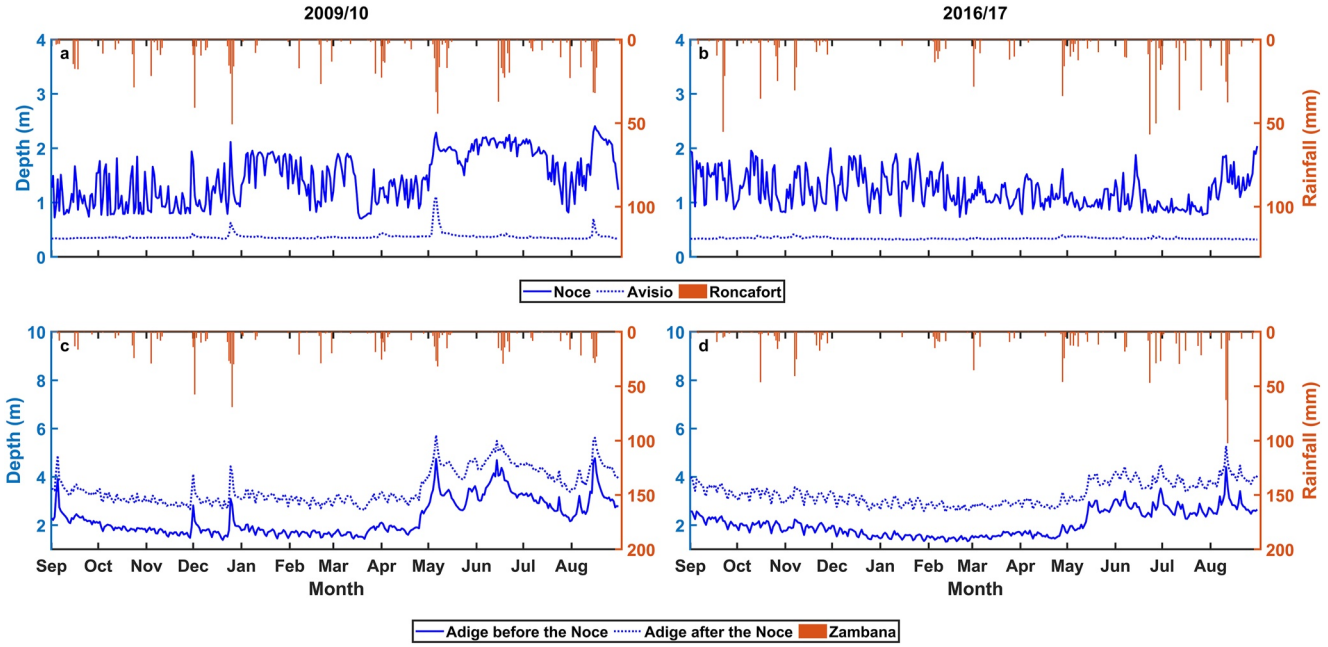

Figure 2. Depiction of river depth (m) time series for the Noce River (a, b), the Avisio River (a, b) and the Adige River before and after the confluence with the Noce river (c, d) for the years 2009/10 and 2016/17 (blue, left *y*-axis). Rainfall (mm) time series recorded in Roncafort (a, b) and Zambana (c, d) stations (orange, right *y*-axis).

ditches naturally flows into the rivers, but when these have high levels, dewatering pumps are activated in order to preserve the land from floods. The ditches are also used to distribute water for irrigation during dry periods through the combined use of gates and inflow from the Noce River.

2.1. Data Collection and River Characteristics

Groundwater head data is collected in collaboration with the Geological Survey of the Autonomous Province of Trento. These data series include 16 manual and 2 automatic measurement points for the period September 2009 to August 2010 and 16 manual and 4 automatic measurement points for the period September 2016 to August 2017 (Figure 1c). Manual data is measured about every 3 months, while automatic data about every 6 hours.

We obtain daily precipitation and temperature data from September 2009 to August 2010 and from September 2016 to August 2017 from the Meteorological Survey of the Autonomous Province of Trento (www.meteotrentino.it) and from 3Bmeteo (www.3bmeteo.com) at the meteorological stations in San Michele all' Adige, Roveré della Luna, Trento (Aeroporto), Zambana - Idrovora, Mezzolombardo - Maso delle Part and Trento - Roncafort (see Figures 1b and 2). It is noteworthy to observe the significantly lower precipitation in 2016–2017 compared to 2009–2010, particularly for October-March (see also Chiogna, Skrobanek, et al., 2018). For example, in that period, the cumulative precipitation decreased around 20% and 30% in the stations of Roncafort and Zambana, respectively.

For the river discharges, we use collected data in the gauging stations of San Michele all'Adige (Adige River, northern part), Trento Ponte San Lorenzo (Adige River, southern part), Lavis (Avisio River) and Mezzolombardo (Noce River) by the Dams Office of the Province of Trento (www.floods.it). The location of the gauging stations is shown in Figure 1b. River discharges at the Adige San Michele gauging station were not available for the 2016/2017 years, and therefore a rating curve has been reconstructed considering river stages and discharges in the hydrological year 2009/10. With a mean streamflow of 46 m^3/s at Mezzolombardo, the Noce River streamflow is highly variable due to the proximity of the Mezzocorona hydropower plant, about 9.3 Km upstream from its confluence with the Adige River (Figure 1b). In general, the Noce River basin (basin area of 1,360 km^2; main course length of 105 km) is highly impacted by hydropower production at different locations (Chiogna et al., 2016; Majone et al., 2016). The northern part of the Adige River reach shows less variability in

the river stage than the Noce river since the operation of hydropower plants is located several kilometers upstream (Chiogna, Marcolini, et al., 2018; Pérez Ciria et al., 2019). However, in the southern part of the Adige River (mean of 212 m³/s at the Ponte San Lorenzo gauging Station in Trento), it is possible to observe the effect of the waves propagating from the Noce River (Pérez Ciria et al., 2019; Zolezzi et al., 2009). Finally, although the Avisio River (mean water discharge of 23.5 m³/s at Lavis) is also exploited for hydropower production, it does not display sharp and regular river stage fluctuations in the study area. Therefore, we consider this river reach as a non-impacted by hydropeaking.

The maximum allowed abstraction rates of all wells present in the study area are provided by the Geological Survey of the Province of Trento. We use these values to calculate the average daily pumping rates used in the model.

This work seeks to establish a proof of concept on how reservoir and hydropower plant operations can affect Alpine aquifers depending on the frequency of water release as well as on the season and on the wet/dry conditions of a specific hydrologic year. Therefore, we apply a single realization of the hydraulic conductivity field (see Figure S1 in Supporting Information S1) rather than multiple realizations. Such conductivity field was obtained from the estimations of Castagna et al. (2015) and had the minimum mean absolute error when compared to the available observations. We acknowledge, however, that hydraulic conductivity is an important source of uncertainty that has to be considered for further studies where uncertainty quantification is relevant.

3. Numerical Model

The Adige aquifer is modeled with MODFLOW-2005 (Harbaugh, 2005), which is a modular finite-difference flow model that solves the groundwater flow equation. We apply the transient groundwater flow model developed by Castagna (2017), based on the calibration of the steady-state model version (Castagna et al., 2015), which is currently the official model applied by the Geological Survey of the Autonomous Province of Trento for their investigations. The transient model assumes the same hydrological parameters as the stationary model, while the forcing factors (river stage, precipitation, evapotranspiration, transient boundary conditions and pumping rate of wells) are transient. The spatial grid of the model (x × y × z) is 80 × 80 × 5 m. The model includes 8 layers, 107 rows and 50 columns, and the total area of active cells is approximately 18 km^2 (Figure 1c).

We analyse two time periods: the first one is from September 2009 to August 2010 and corresponds to a wet year; the second one is from September 2016 to August 2017 and represents a dry year. While variability in the operation of hydropower plants also occurs at the subdaily scale (Perez Ciria et al., 2019; Zolezzi et al., 2011), we consider a daily temporal resolution since it allows us to describe the 7 days' periodicity in the aquifer, which is the focus of this work.

The time series of four piezometers are used to define the boundary conditions of the groundwater model, implemented as Time-Variant Specified-Head (CHD) Package (Harbaugh, 2005). These piezometers are: piezometer 348 for the north side close to the Noce River, piezometer 39 for the north side close to the Adige River, piezometer 134 for the south-east side, and piezometers 218 and 580 for the south-west part in the hydrological years 2009/10 and 2016/17, respectively (Figure 1c). This change in the modeling of the two hydrological years is needed due to the available data. We present an extended description of the head boundary conditions in Text S1 in the Supporting Information S1.

To implement the river-groundwater interaction, we apply the river (RIV) package (Harbaugh, 2005). The flow between surface water and groundwater q_{riv} [L^3/T] is modeled according to the following equation (Harbaugh, 2005):

$$\begin{aligned} q_{\text{riv}} &= C_{\text{riv}}(H_{\text{riv}} - h) \text{ if } h > R_{\text{bot}} \\ q_{riv} &= C_{riv}(H_{riv} - R_{bot}) \text{ if } h \leq R_{bot} \end{aligned} \quad (1)$$

where C_{riv} [L^2/T] is the hydraulic riverbed conductance, H_{riv} [L] is the water stage of the river, h [L] is the groundwater head simulated by MODFLOW below the river reach cell, and R_{bot} [L] is the bottom of the riverbed. q_{riv} is positive if the water flows from the river to the aquifer, and negative if vice versa. The values of H_{riv} are obtained in the output of a hydraulic simulation performed with the Software HEC-RAS (U.S. Army Corps of Engineers, 2016), which is calibrated and validated based on the collected daily river discharge (Section 2.1).

Figure 2 (left axis) displays the computed daily river stages for the years 2009/10 and 2016/17 in the cells close to the model observation points near the rivers (Figure 1c).

Hydraulic parameters (riverbed conductance, hydraulic conductivity, and river bottom) were estimated in Castagna et al. (2015) and Castagna (2017) using the inversion of hydraulic head data by applying the Particle Swarm Optimisation (PSO) Algorithm (Robinson & Rahmat-Samii, 2004). The calibration process is found in Castagna et al. (2015), and additional details on the generation of the heterogeneous hydraulic conductivity field appears in Text S2 in the Supporting Information S1.

The infiltration into the saturated zone is implemented using the Recharge (RCH) package (Harbaugh, 2005), which assigns values to each grid cell of the shallowest layer. In order to estimate the recharge to the aquifer, we apply the leakage model (Rodríguez-Iturbe & Porporato, 2007) used in Castagna et al. (2015). This model considers that recharge depends not only on the precipitation, but also on irrigation, evapotranspiration and the soil characteristics (e.g., soil moisture). For the precipitation, we used the daily rainfall values collected by the meteorological stations (Figure 1b). The wavelet power spectrum of these time series is provided in the Supporting Information S1 (Figure S2) and shows that high power is present during the events and propagates over several temporal periods as already observed for example, by Bittner et al. (2021) and Schaefli et al. (2007). The irrigation rate is obtained based on the observations of Toller (2002). To calculate the evapotranspiration we follow the Thornthwaite Method (Chen et al., 2005; Sacratees, 2017). The soil characteristics are based on the work by Laio et al. (2001). We use the Voronoi triangulation as spatial aggregation method and therefore we assigned irrigation and precipitation to the model cells according to Thiessen polygons. Finally, we set the leakage to zero in urban areas. A complete description of the leakage model and the estimation of irrigation and evaporation rates are found in the Supporting Information S1 (Text S3 and S4, respectively).

The well withdrawals provided by the Geological Survey of the Province of Trento are inserted into the model as punctual discharge rates, by applying the Well (WEL) package (Harbaugh, 2005). The pumping rates were calculated depending on the monthly irrigation demand and applied as daily average values. Further details about the implementation of extraction wells are provided in the Supporting Information S1 (Text S5). The implementation of the ditches network was also done using the river package. Additional details are found in the Supporting Information S1 (Text S6).

The model results are compared to head data available for continuous monitoring data collected in piezometers 349 and 411 in 2009/2010 and in piezometers 343, 349, 559 and 560 in 2016/17. The R^2 obtained is 0.997 and 0.991 for the two hydrological years respectively. Moreover, the results are compared with manual data provided by the Geological Survey of Trento and collected at the piezometers available in the study area (Figure 1c). Considering also these manual data, R^2 is 0.987 for the year 2009/10 and 0.990 for the year 2016/17.

4. Wavelet Analysis

The goal of the continuous wavelet transform (CWT) analysis is the detection of periodicity in a signal and the determination of the temporal scales and time period at which they are dominant (Agarwal, Maheswaran, Kurths, & Khosa, 2016; Agarwal, Maheswaran, Sehgal, et al., 2016; Pérez Ciria et al., 2019; Torrence & Compo, 1998). The CWT is defined as the convolution of a continuous signal with a scaled and translated version of the mother wavelet function $\psi(t)$. In the case of a discrete sequence x_n with a time step δt, where n indicates the localized time index, the CWT is approximated as:

$$W_n(s) = \sum_{n'=0}^{N-1} x_{n'} \psi^* \left(\frac{(n' - n)\,\delta t}{s} \right), \tag{2}$$

where $(*)$ indicates the complex conjugate, n' is the time variable, s is the wavelet scale and N is the number of points in the time series (Torrence & Compo, 1998). In the present work, the Morlet mother wavelet function is chosen for its good compromise between time and frequency resolution (Grinsted et al., 2004; Pérez Ciria & Chiogna, 2020; Schaefli et al., 2007). It is defined as

$$\psi(t) = \pi^{-1/4} e^{i\omega t} e^{-t^2/2}, \tag{3}$$

where t is the dimensionless time and ω is the dimensionless angular frequency. In our calculations ω is set to 6 (Grinsted et al., 2004), since this number provides a good balance between time and frequency localization, while the scale value s in Equation 2 is a fractional power of 2. Since the analyzed time series have a finite length, the wavelet analysis is affected by edge effects. The area where these effects become important is defined as the cone of influence (Torrence & Compo, 1998).

4.1. Wavelet Transform Coherence

The wavelet transform coherence (WTC) allows us investigating the local correlation between two CWTs (Pérez Ciria & Chiogna, 2020). It is defined as (Torrence & Webster, 1999):

$$R_n^2(s) = \frac{\left|S\left[s^{-1}W_n^{XY}(s)\right]\right|^2}{S\left[s^{-1}\left|W_n^X(s)\right|^2\right] S\left[s^{-1}\left|W_n^Y(s)\right|^2\right]}, \tag{4}$$

where S is the smoothing operator, given by $S(W) = S_{\text{scale}}\{S_{\text{time}}[W_n(s)]\}$, while S_{scale} denotes smoothing with respect to scales s and S_{time} smoothing in time. WTC varies between 0 (uncorrelated) and 1 (fully correlated). This definition is similar to that of the correlation coefficient and the WTC can be interpreted as a localized correlation coefficient in the time-frequency space (Grinsted et al., 2004). We further consider two additional metrics to evaluate the model performance. The first one is the mean coherence between model and continuously available groundwater head data (in 2009/10 piezometers 349 and 411, and in 2016/17 piezometers 343,349,559 and 560) computed over the entire simulation time and all periods. The second one is the mean coherence between model and continuously available groundwater head data computed over the entire simulation time and only the 7-days period (Chiogna, Marcolini, et al., 2018). In both cases, we obtain a mean coherence value of 0.7

4.2. Wavelet Maps

Continuous wavelet transform informs about the strength of a periodic signal for a specific periodicity and a specific time. Beside this information, we are interested in quantifying the average behavior of the groundwater table during the year and hence we compute the normalized time-average of the wavelet spectrum $\overline{W_n(s)}$, as

$$\overline{W(s)} = \frac{\left(\frac{1}{N}\sum_{n=0}^{N-1}|W_n(s)|^2\right)}{\sum_s\left(\frac{1}{N}\sum_{n=0}^{N-1}|W_n(s)|^2\right)}. \tag{5}$$

In order to visualize the spatial variability of this value for the 7-days period, we create the matrix $\overline{W(7)}$, where each element corresponds to the normalized time-averaged wavelet spectrum of the hydraulic head in the corresponding cell of the domain for a weekly signal:

$$\overline{W^{ij}(7)} = \frac{1}{N}\sum_{n=0}^{N-1} W_n^{ij}(7), \tag{6}$$

where the superscript ij refers to the cell (i, j) in the model, $W_n^{ij}(7)$ corresponds to the value of the wavelet spectrum for the hydraulic head at the time step n and for the period of 7 days.

We apply a similar procedure for the wavelet coherence. In this case, each element of the matrix $\overline{C(7)}$, corresponds to the average of the coherence wavelet between the river stage and the hydraulic head computed for each cell over time at a 7-days period,

$$\overline{C^{ij}(7)} = \frac{1}{N}\sum_{n=0}^{N-1} R_n^{2\,ij} \tag{7}$$

giving hence a sort of mean coherence correlation along the year. The wavelet analysis and related elaborations have been performed with the Software MATLAB R2020b.

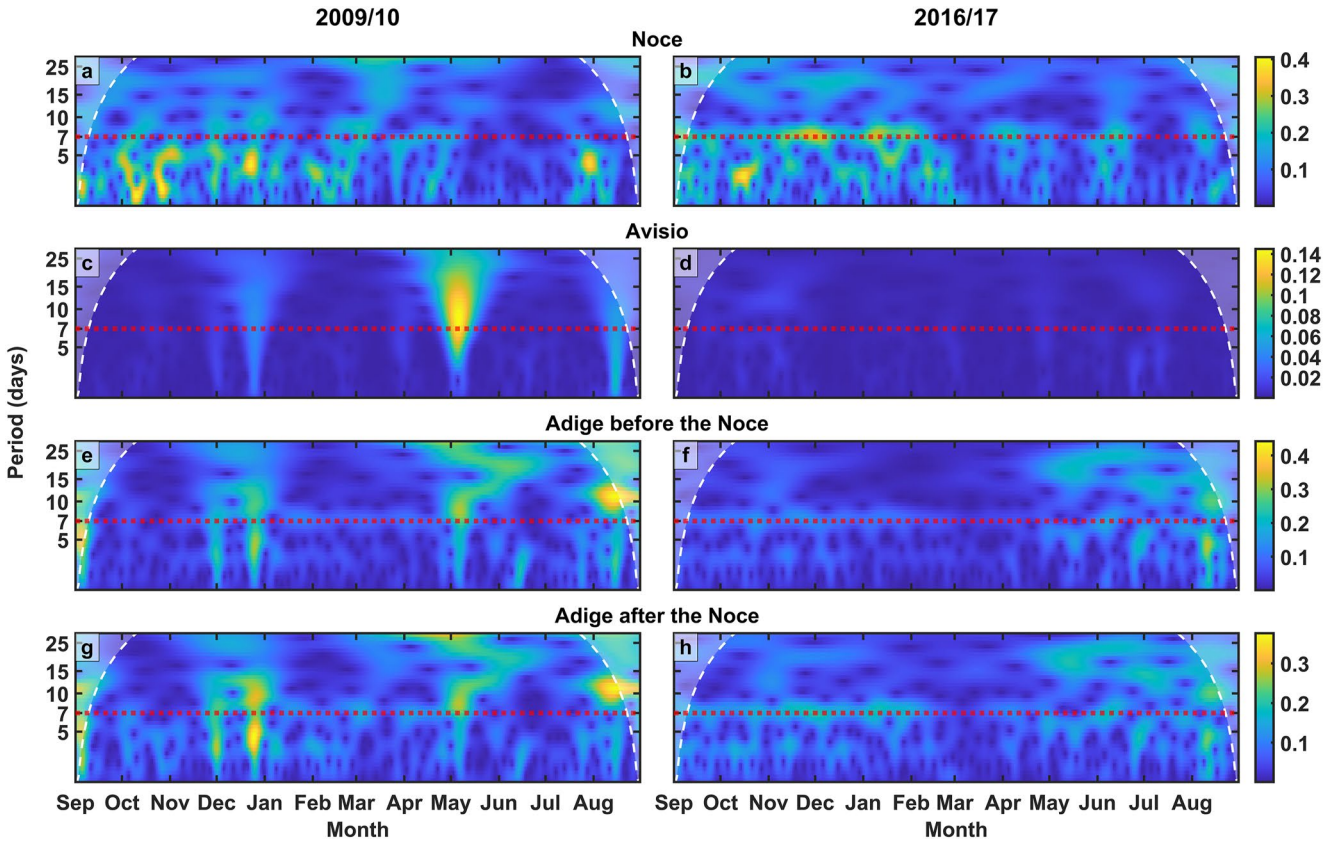

Figure 3. Continuous wavelet transform of the river's stage time series. Warmer color indicates times and periods of intense power. The white shaded areas show the cone of influence. The dashed red line along the period of 7 days identifies the temporal scale focus of the present study.

5. Results

5.1. Variability in the River Stages

We analyze the influence of hydropower plant operations in the rivers by computing the continuous wavelet transform of the river stage time series shown in Figure 2, where the withe shaded area represents the cone of influence.

The continuous wavelet transforms presented in Figure 3 show considerable variations in high power regions across the river stage time series of the two hydrological years (2009/10 and 2016/17, respectively) for the Noce, Avisio, and Adige before and after the confluence with the Noce.

A light (yellow) color indicates times and periods of intense signal. The red dashed line in Figure 3 helps to identify the level of 7-days periodicity. Therefore, a higher intensity along this dashed line is an indicator of weekly streamflow alteration associated to low energy production during weekends (i.e., low stage in the affected rivers during the weekends and high stage during the week). In addition, high powers spreading over different levels of periodicity at a specific time are an indicator of intense precipitation events, as also observed by Schaefli et al. (2007). In our study area, large precipitation events generate a peak in the power spectrum from periods of 2 days until about 15 days as it can observed for example, for the events occurred on December 1, 2009, December 25, 2009, and May 6, 2010. However, time series over longer periods may show coherence between precipitation and groundwater fluctuations that are not associated to specific rainfall events (e.g., Dountcheva et al., 2020).

The Noce River displays a peak in the power spectrum at the weekly scale typical for Alpine rivers affected by storage hydropower plant management (Chiogna, Marcolini, et al., 2018; Pérez Ciria et al., 2019) stronger during the wintertime, that is, under low flow conditions, for both the hydrological years. We can also observe that the signal is stronger and more persistent in the snow scarce year 2016/17 (Chiogna, Skrobanek, et al., 2018) than in

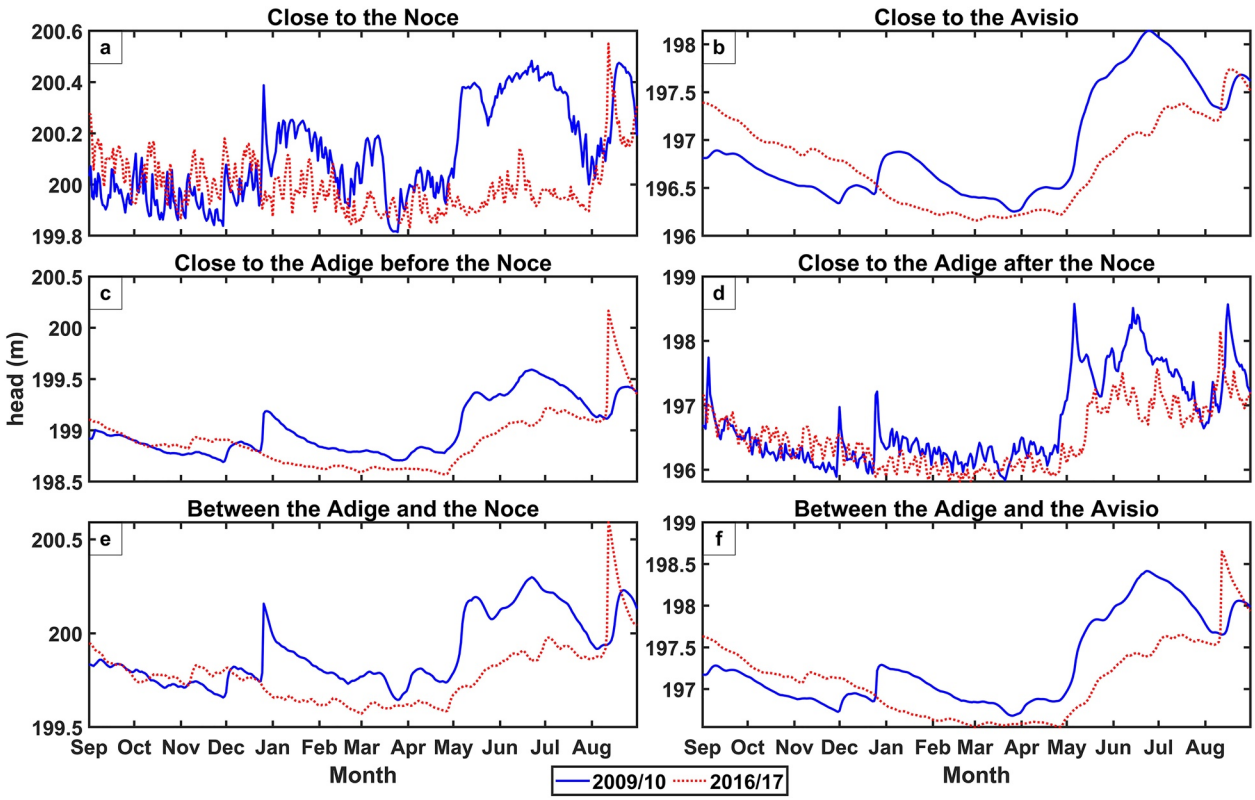

Figure 4. Simulated groundwater heads [m] at six selected locations (see Figure 1c) namely (a) close to the Noce, (b) close to the Avisio, (c) close to the Adige before the Noce, (d) close to the Adige after the Noce, (e) between the Adige and the Noce, and (f) between the Adige and the Avisio for the hydrological years 2009/10 (blue solid line) and 2016/17 (red dotted line).

2009/10 since it extends to the spring period due to the lack in groundwater recharge due to snowmelt. Moreover, since the river stage is determined mainly by the hydropower plant operation, we do not observe significant impact of precipitation events in the power spectrum. High power values at the weekly period are also present in the whole analyzed segment of the Adige, even though it is stronger after the confluence with the Noce river. Furthermore, the Adige stage time series display peaks in the power spectrum induced by the precipitation events of December 2009 and May 2010, since the river stage is not only influenced by hydropower plant operation. These signals are also observed in the Avisio River, where we do not detect the 7-days periodicity due to surface water management operations.

5.2. Variability in the Simulated Groundwater Heads

To analyze the temporal variability of the groundwater table, we select six representative locations in the computational domain, indicated in Figure 1c. Four points are distributed in the domain to capture the behavior of the aquifer close to the rivers (close to the Noce River, close to the Avisio River, close to the Adige River before its confluence with the Noce and close to the Adige River after its confluence with the Noce), while two points represent the aquifer not influenced by the rivers (between the Adige and the Noce rivers and between the Adige and the Avisio rivers).

Figure 4 shows time series of the groundwater head at the six selected locations within the computational domain for the two considered hydrological years of 2009/10 and for 2016/17. We can observe that close to the Noce River (Figure 4a) the groundwater level displays rapid fluctuations of small amplitude throughout the year. This result contrasts with the observations for the groundwater head simulated close to the Avisio River, where the hydraulic head smoothly varies during the year, with higher water table in spring and summer when groundwater recharge occurs (Figure 4b). Far from surface water bodies, that is, between the

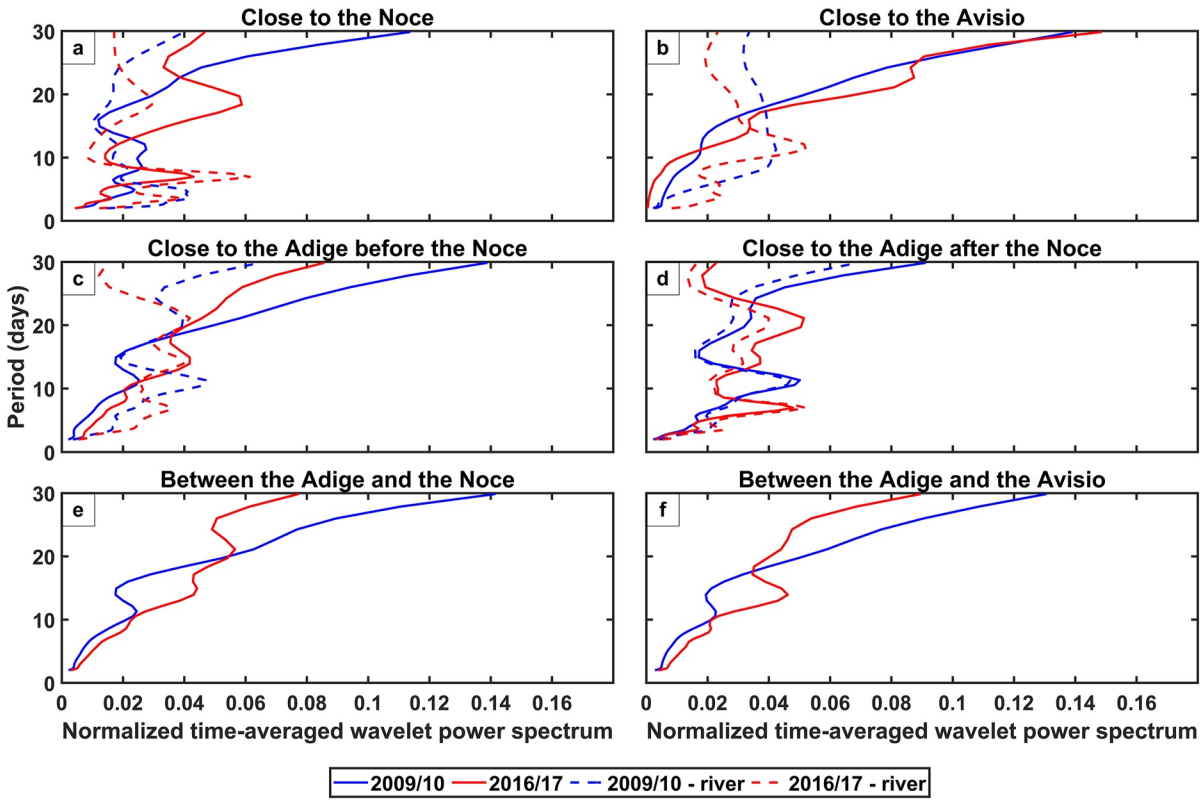

Figure 5. Normalized time-averaged spectrum of the groundwater estimated at six selected locations (see Figure 1c), namely (a) close to the Noce, (b) close to the Avisio, (c) close to the Adige before the Noce, (d) close to the Adige after the Noce, (e) between the Adige and the Noce, and (f) between the Adige and the Avisio for the hydrological years 2009/10 (blue solid line) and 2016/17 (red solid line). (a–d) also shows the normalized time-averaged spectrum for the river depth closest to the observation points for the years 2009/10 (blue dashed line) and 2016/17 (red dashed line). In (a) river refers to the Noce, in (b) river refers to the Avisio, and in (c and d) river refers to the Adige.

Adige and the Noce rivers (Figure 4e) and between the Adige and the Avisio rivers (Figure 4f) the aquifer behaves similar to the point close to the Avisio River. Particularly interesting are the results obtained for the Adige River where the surface water fluctuations in the riverhead of the Adige River before the confluence with the Noce are not strong enough to clearly propagate into the aquifer (Figure 4c). However, the impact of the Noce River on the Adige River is evident also in the aquifer and in fact after the confluence with the Noce also the aquifer close to the Adige River is characterized by fluctuations caused by surface water management (Figure 4d). Noteworthy is the reduced or even absent groundwater head increase in 2016/17 in the spring/summer period due to the lack of intense precipitation events as well as of snow melt occurred in that season.

We calculate the normalized time-averaged wavelet power spectrum according to Equation 5 (Figure 5) in order to analyze the overall behavior of each period integrated over time. For the groundwater observation points close to a river, we include in the figure the time-averaged wavelet power spectrum for the respective river depth, that is, the Noce River (Figure 5a), the Avisio River (Figure 5b), and the Adige River (Figures 5c–5d). In such locations, we see that the behavior of the time-averaged wavelet power spectrum is similar between the river and the groundwater (Figures 5a–5d), in particular in case of the Noce and Adige rivers. With respect to the different hydrological years, we can observe that in 2016/17 the period of 7 days displays a sharp peak for the Noce and the Adige after the Noce observation points (Figures 5a and 5d), while the Adige before the Noce, the Avisio and the points far from the influence of the rivers display a broad peak at about 15 days (Figures 5b, 5c, 5e–5f) which can be associated mainly to recharge processes due to precipitation or their overlap with the signal caused by surface water management. In the year 2009/10, the weekly peak is less evident also for the Noce and the Adige after the confluence due to the more intense and frequent

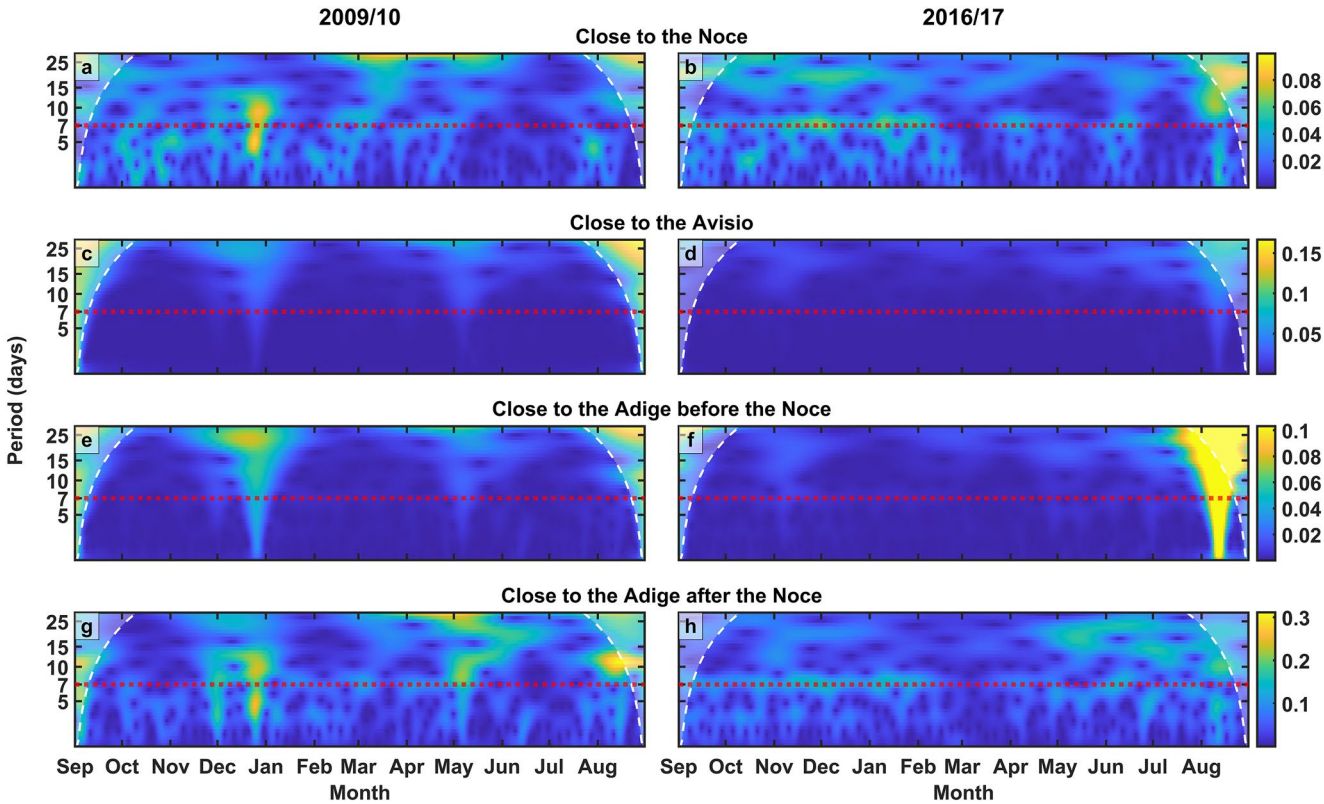

Figure 6. Continuous wavelet transform of the groundwater head time series at selected locations (see Figure 1c). Warmer color indicates times and periods of intense power. The white shaded areas show the cone of influence. The dashed red line along the period of 7 days identifies the temporal scale focus of the present study.

precipitation events in that year, since they generate very high power values over several periods. To see how the weekly signal changes over the time, we additionally show the weekly wavelet coherence between the groundwater at the selected locations and the closest river in Figure S3 of the Supporting Information S1. This analysis however provides only a partial representation of the complexity of the interaction between surface water and groundwater in this system, since it does not allow us to investigate the non-stationarity in the power spectrum.

Figure 6 presents the wavelet power spectrum of the groundwater heads at the four selected locations closer to the rivers. The observation point close to the Noce River has the highest power at the period of 7 days for both hydrological years (Figures 6a and 6b). In particular, during the autumn and winter months, signal persistence in 2016/17 is higher than in 2009/10. Therefore, we can observe that the weekly wavelet signal is stronger in the aquifer during low flow periods. The low flow periods can be caused by the typical lack of groundwater recharge in the autumn and winter months, or due to a particularly dry winter, which - since the catchment is snow dominated - leads to little snow accumulation and thus to a lack of spring recharge (as for the 2016/17 years). This explains why the normalized time-averaged wavelet spectrum displays a sharper peak at a weekly period in 2016/17 than in 2009/10 (Figure 5a). The Avisio River does not display the 7-days periodicity neither in the river (Figures 3c and 3d) nor in the groundwater (Figures 6c and 6d). Despite the weekly signal present in the Adige River before its confluence with the Noce (Figures 3e and 3f), the groundwater near the river (Figures 6e and 6f) does not show this periodicity. This is most likely due to the interplay between the forcing signal and the hydraulic properties of the riverbed and the aquifer. Close to the Adige after the Noce, the continuous wavelet spectrum of the groundwater (Figures 6g and 6h) behaves similar to the groundwater near the Noce. However, the values in the power spectrum at the period of 7 days are smaller. This periodic signal has an anthropogenic nature and it is caused by the impact of water management for hydropower production on the river stage. Overall, the analysis of the continuous wavelet power spectrum and the normalized time-averaged wavelet power spectrum confirm the distinct difference between wet and dry years.

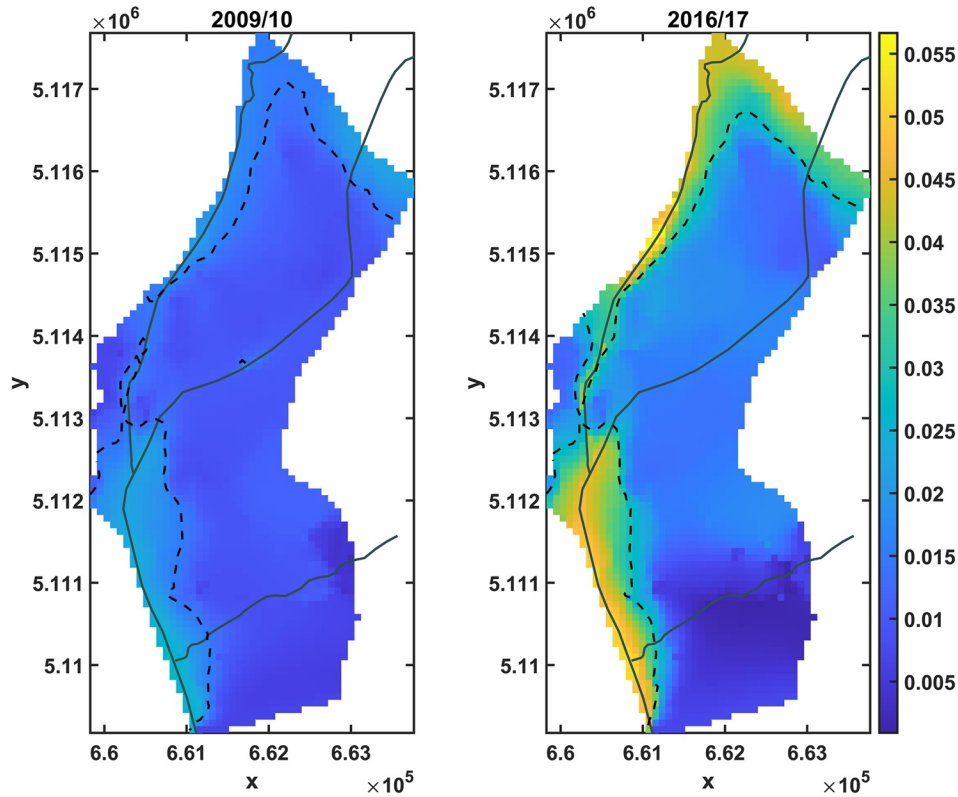

Figure 7. Map of the normalized time-averaged wavelet spectrum at a period of 7 days for the years 2009/10 and 2016/17. Warmer color indicates areas of higher power spectrum intensity. The dashed black lines show the area above the 75th percentile. Solid lines depict the rivers.

5.3. Maps of Wavelet Spectrum and Coherence Wavelet Between River Stage and Groundwater Heads

Figure 7 shows a map of the normalized time averaged wavelet spectrum value at the weekly period to extend the results obtained for the six observation points in Figure 5 to the entire study area. Here, higher values indicate that the 7-day averaged signal (understood as impact on the aquifer of the streamflow alteration due to hydropower plant operations) is more intense for that specific location in comparison to other cells in the domain. In general, the power spectrum is lower in 2009/10 than in 2016/17, confirming that the impact of hydropeaking on the aquifer is more severe in a dry year than usual. Furthermore, the zones above the 75th percentile of the power spectrum intensity in each map are delimited with a dashed line to better identify the most influenced areas. In both years, we can consistently observe high values (above the 75th percentile) of the wavelet power close to the Noce River and close to the Adige after its confluence with the Noce. Notice that the results of the northern boundary condition are likely affected by the piezometer used to define the constant head boundary condition and therefore should be carefully interpreted (see Text S1 in the Supporting Information S1).

To quantify the area of the aquifer affected by surface water management, we calculate the time-averaged wavelet coherence between the simulated groundwater level and the river stage in the closest river cell at the period of 7 days as given in Equation 6. The resulting maps are shown in Figure 8, where we observe high coherence between river stages and groundwater heads in both the hydrological years. High coherence values are distributed over a larger area for the year 2009/10 compared to that of 2016/17. This is because precipitation events affect both the river stage and the aquifer also in locations where there is no groundwater-surface water interaction. However, in both years, the highest coherence values occupy the portion of the aquifer closer to the rivers affected by hydropeaking.

The intensity of the signal and the extension of the impacted area depend on landscape attributes such as hydraulic conductivity, saturated thickness of the aquifer and specific yield. However, a systematic analysis is difficult to be performed in a real case study like the one considered in this study since the hydraulic conductivity field is

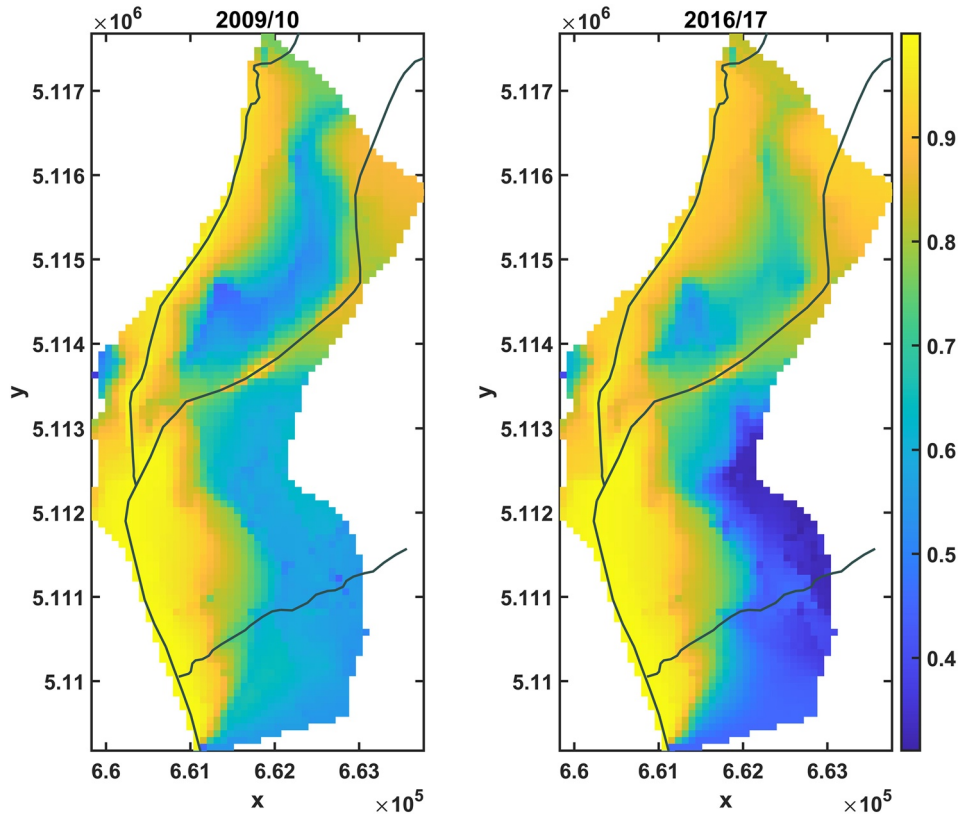

Figure 8. Map of the time-averaged coherence wavelet spectrum at a period of 7 days for the years 2009/10 and 2016/17. Warmer color indicates areas of higher coherence between the river stage and groundwater heads. Solid black lines depict the rivers.

heterogeneous in all three spatial dimensions and this influences the wave propagation in a non-trivial way. Moreover, the presence of the ditches can dampen the propagation of the signal, in particular during the wet periods when they can receive more water from the aquifer since the water exchange is proportional to the groundwater head. However, as we can observe by comparing Figures 1c and 8, high coherence values also appear beyond the area occupied by the ditches. Furthermore, groundwater abstraction may also have a local effect on the analysis although it is of minor importance. In fact, the pumping rate of the wells does not occur with a specific temporal frequency that could interfere with the river signal and the pumping rates only affect areas which are small compared to the grid area of the model (80 × 80 m).

5.4. Exchange Fluxes Between Rivers and the Groundwater

Finally, we analyze the flux exchanged between the river reaches and the underlying groundwater cells. We calculate with the Software Zonebudget (Harbaugh, 1990) and the Python-package FloPy (Bakker et al., 2016) the water budget over the area surrounding the rivers (3 cells to the right and 3 to the left of each river cell corresponding to 240 m in each direction) considering separately the Adige River before merging with the Noce, the Adige River after merging with the Noce, the Noce River and the Avisio River. The Noce River mostly feeds the aquifer without strong seasonal patterns, although the exchanged water volume is lower in the dryer year (Figures 9a and 9b). The Avisio River is always feeding the aquifer, with clear peaks during the raining events of 2009 (Figures 9c and 9d). In Figure 9e, we observe that before the confluence with the Noce, the aquifer mainly feeds the Adige River until end April for the year 2009/10; then, the river has intermittent time intervals, in which it feeds the aquifer, in particular those associated with precipitation events. In the year 2016/17, the behavior of water exchange for the same reach is similar, although peak of water going to the aquifer is lower (Figure 9f). After the Adige merges with the Noce, the groundwater predominately feeds the river (Figures 9g and 9h), and

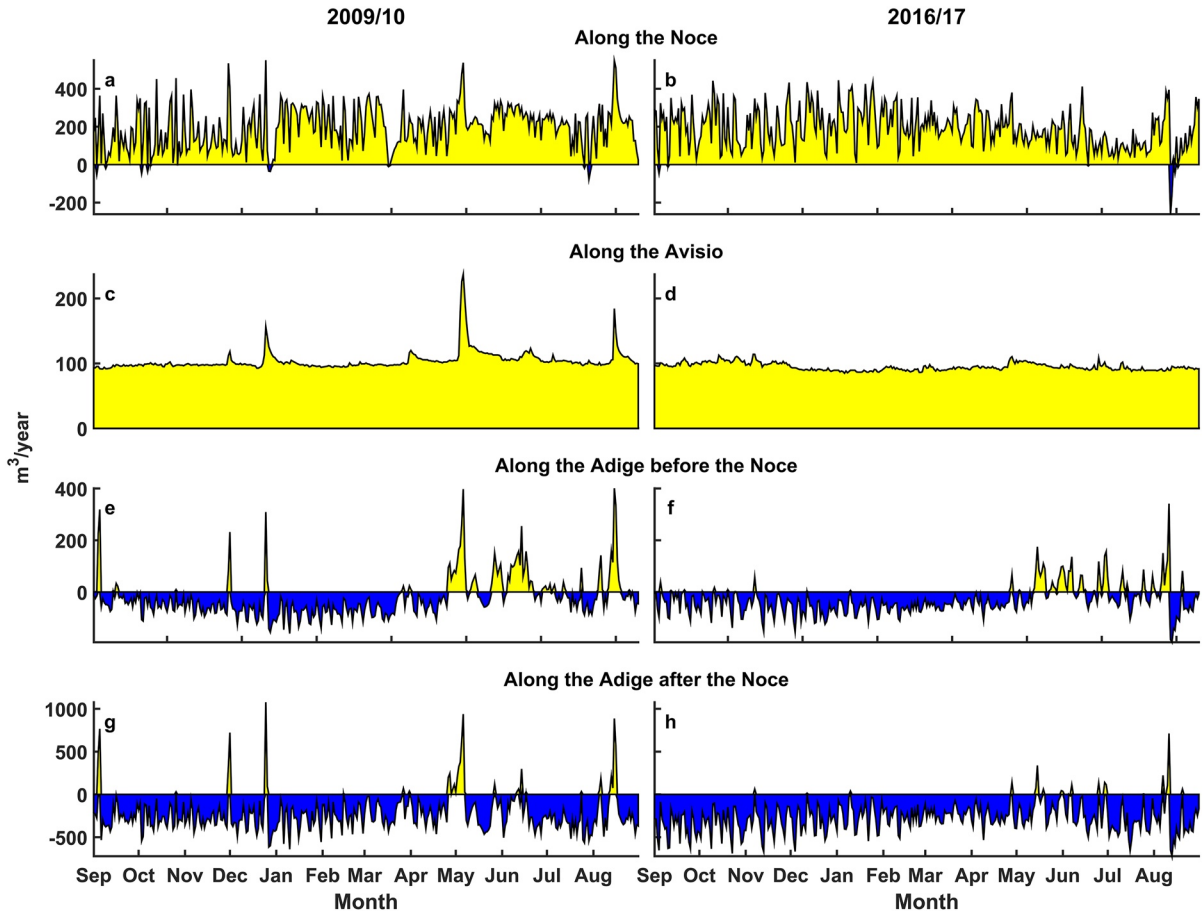

Figure 9. Water budget along the Noce, the Avisio, the Adige before the Noce and the Adige after the Noce. Negative values (blue areas) mean that the aquifer is feeding the river, positive values (yellow areas) mean that the river is feeding the aquifer.

while at intermittent time intervals, the water flux changes direction, the amount of water going from the river to the aquifer is much lower than that before the confluence with the Noce.

To analyze the periodicity of the exchange fluxes, we estimate the normalized time-averaged power spectrum of the difference between the water entering and leaving the system for each river (Figure 10). For the year 2009/10 we observe a clear peak around 4-days period along the Adige and the Noce Rivers. This peak is also associated to water management operations (Perez Ciria et al., 2019) and is characteristic for high flow condition during five working days and low flow conditions over the weekend. The 4-day peak also appears in the year 2016/17; however, that year displays an additional and dominating peak around the weekly period. This shows that although the volume of exchanged water does not significantly change in dry and wet years (Figure 9), the temporal dynamics of these exchanges is affected and may therefore impact solute and thermal transport.

6. Discussion

6.1. Wavelet Analysis for Understanding Highly Managed River Systems

The specific study area of this study includes four river reaches differently influenced by hydropower plant operations. As shown in Figure 3, despite the similar hydrometeorological and climatic conditions, the composition of the river signal shows a strong difference, highlighting the dominant impact of water management on streamflow. Furthermore, thanks to the peculiarity of the investigated region, we are able to analyze the aquifer's response in two different years (2009/10 and 2016/17) with different hydrological and surface water management conditions. When we apply continuous and coherence wavelet analysis to study groundwater-surface water interactions, we observe a stronger impact of the river weekly signal on the aquifer during dry periods than during wet periods.

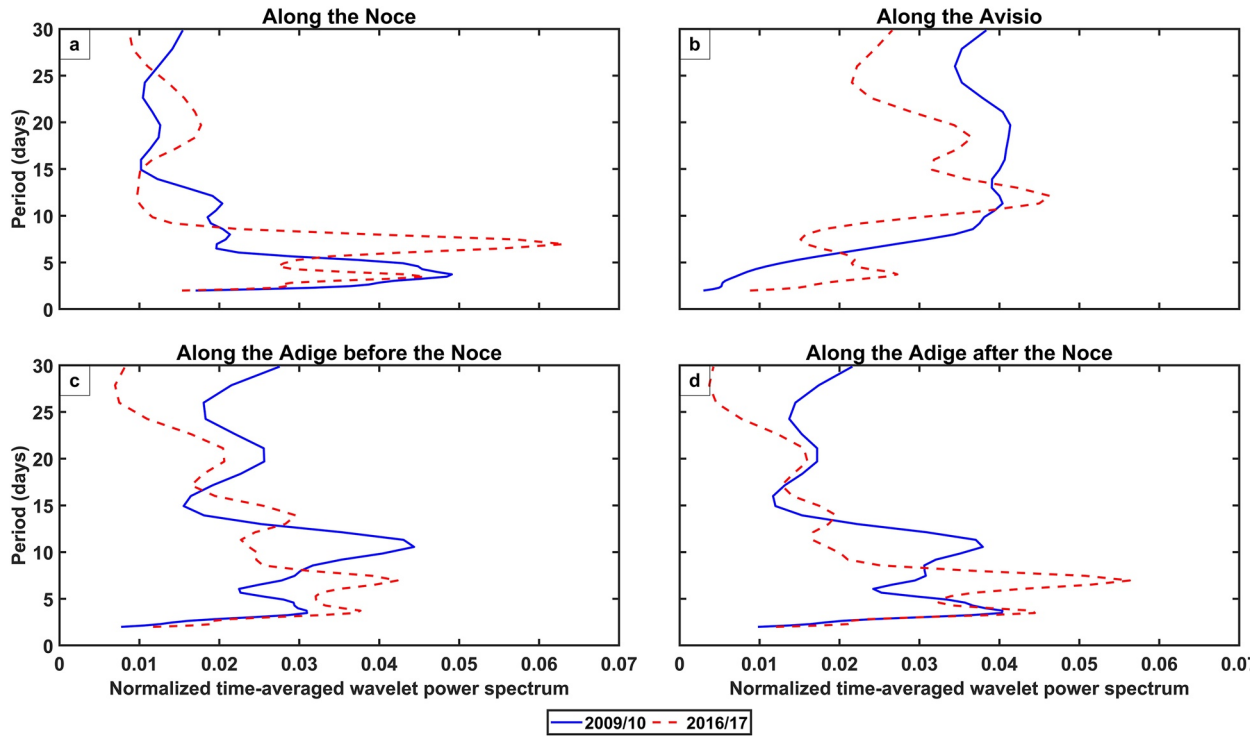

Figure 10. Normalized time-averaged power spectrum of the water budget along Adige, the Avisio, and the Noce.

Our findings are in line with the outcomes of Song et al. (2018) for the Columbia River and its underlying aquifer, as well as Li and Pasternack (2021), who analyzed several rivers in the state of California, most of them originating in Sierra Nevada and with a summer base flow controlled by snowmelt. Both authors pointed out that drought conditions can lead to stronger impacts from hydropeaking. However, while Song et al. (2018) focused on the hyporheic exchange, Li and Pasternack (2021) analyzed the river regimes. They concluded that the annual frequency of hydropeaking was higher in the dry season and in dry years compared to the wet season and wet years because of changes in the operation of hydropower plants (i.e., hydropower facilities generate electricity constantly since there is sufficient water). In our study, we observe that changes in the groundwater level fluctuations observed during the drier year 2016/17 respond to both the aquifer recharge (depending on meteorological conditions and soil properties) and to the surface water fluctuations, in particular in areas closer to the rivers. Since the surface water fluctuations com from river stage measurements, they already account for both precipitation events and, if it is the case, for changes in the operation of hydropower plants.

The continuous wavelet analysis (Figure 3) and the normalized time-averaged wavelet power spectrum analysis (Figure 5) show no significant signal at the 7-days periodicity in the aquifer close to the Avisio River, which is not affected by dam operations. In contrast, the signal isclearly visible in rivers affected by dam operations, such as the Noce River, and is more evident in low flow conditions, such as winter months or dry years. The groundwater close to these rivers shows a similar behavior (Figures 6a, 6b, 6g, and 6h), indicating how the management of hydropower plants, especially in dry years, can affect the aquifer. The continuous wavelet analysis does not display any strong weekly signal at the observation point close to the Adige before the Noce (Figures 6e and 6f), even though the signal is present in the river stage fluctuations of the Adige in its proximity (Figures 3e and 3f). Two factors may explain this behavior: first, the signal in the river is weaker than the one observed after the confluence with the Noce River or in the Noce itself. Second, the porous material of the aquifer acts as a filter for the propagation of the fluctuations For instance, in a heterogeneous aquifer the signal of a fluctuating river dampens closer to the river in areas of low hydraulic conductivity (Merchán-Rivera, Basilio Hazas et al., 2022), as occurs in the aquifer area corresponding to the upstream reach of the Adige River. Moreover, other factors such as the specific yield and aquifer thickness also play a role in the propagation of the signal into the aquifer (Sawyer et al., 2009).

Finally, we would like to highlight the importance of weekly fluctuations to study the aquifer at the regional scale. As mentioned in Section 3, the operation of hydropower plants in the Adige catchment also happens at the subdaily scale, with important implications to the ecological and physical-chemical characteristics of the rivers (Bruno et al., 2013; Zolezzi et al., 2011), and eventually to the transport of contaminants in the underlying aquifer (Basilio Hazas & Chiogna, 2022). However, higher frequencies have a shorter propagation distance in the aquifer (Merchán-Rivera, Basilio Hazas et al., 2022; Rizzo et al., 2020; Sawyer et al., 2009) and therefore would have less impact at the scale considered in this work.

6.2. Effect of Hydrological Conditions on Weekly Aquifer Fluctuations

In both years, the aquifer shows stronger 7-day fluctuations close to the Noce River and the Adige River after the confluence with the Noce River (Figure 7). However, the difference in intensity between wet and dry years evidences the hydrological control on the propagation of streamflow alterations in the aquifer system. The time-averaged wavelet coherence on the period of 7-day displayed in Figure 8 is generally higher and distributed on a smaller range for the year 2009/10, when the aquifer is more influenced by the precipitation. The fact that the values in areas far from the rivers or in the Avisio have similar values to the areas close to the Noce and to the Adige after the confluence with the Noce, shows that specific conditions of a hydrological year, such as snow melting or precipitation, can have a larger influence in a wet year over the entire aquifer, blurring the effect of fluctuations due to dam operations. As precipitation and temperature seasonality have the most impact on aquifer recharge (Moeck et al., 2020), in the studied area, precipitation events affect both river discharge and aquifer recharge, and lead to a coherent signal between river stage fluctuations and the groundwater hydraulic head even for aquifer regions not influenced by surface water - groundwater interaction. However, it appears that the extension of the total area displaying coherence values larger than 0.8 is very similar between the two contrasting hydrological situations (around 8 Km^2 in 2009/10, 7 Km^2 in 2016/17). Therefore, while hydrological conditions (wet/dry year) control the intensity (i.e., power) of the period of 7 days, the extension of the aquifer affected by surface water management does not seem to be very sensitive to the same hydrological drivers. These observations indicate that the portion of the aquifer influenced by the river fluctuations is strongly related to their periodicity and the aquifer characteristics itself, which is in accordance with the analytical solution for the head response presented in Sawyer et al. (2009) and Singh (2004).

6.3. Impact of Surface Water Management on Surface Water-Groundwater Exchange Fluxes

The management of the hydropower plants also influences the frequencies of the interactions between river and aquifer, as it is shown in Figure 10 with the normalized time-averaged wavelet power spectrum of the water budget along the four different reaches. Strong peaks at the 7-day frequency are visible along the Noce River and along the Adige River for the period 2016/17 (Figures 10a, 10c–10d), suggesting that dry years may trigger changes in the frequency of the water exchange. In fact, the exchange between surface water and groundwater is controlled by the hydraulic gradient between the two water bodies. Therefore, if the groundwater level is below the average value during dry years, the fluctuations of the surface water bodies have a stronger effect since the minimum head in the river is prescribed by law through the ecological flow (European Commission, 2016), which often depends on habitat suitability index for different species and on economic activities (e.g., Carolli et al., 2017). As the changes are observed in rivers differently affected by hydropower management, these findings highlight the relevance to the weekly period associated with streamflow alteration.

Altered streamflow conditions can either decrease or increase the residence times of the water and solute in the subsurface (Gomez-Velez et al., 2017; Merchán-Rivera et al., 2021; Singh et al., 2019). This is primarily dependent on the specific characteristics of the shape and intensity of the alterations and on geomorphological conditions. Our results further highlight that the seasonal meteorological conditions in a specific hydrological year affect not only surface water management but also surface water-groundwater interaction. Drought conditions induce stronger signal at the periodicity of 7 days, indicating a potential change in the transport of energy, solutes and even contaminants into the aquifer. This change may have implication for the transport of DOC and therefore affect biochemical reactions such as denitrification (Hinton et al., 1997; Inamdar et al., 2004). Apart from biogeochemical implications, surface water management also affects the river-aquifer systems from a thermodynamics point of view as fluctuations in the river stage alter the thermal spatial and temporal patterns in the subsurface (e.g., Song et al., 2018). This effect can be even stronger considering that rivers affected by hydropeaking are also

affected by sudden fluctuations in temperature (Choi & Choi, 2018; Zolezzi et al., 2011). The unregulated dam operations can be thus detrimental to the ecological health status of the river-aquifer systems. Water regulatory agencies should plan the monitoring of dam operations taking precipitation events and groundwater response into account. This would help to better manage the overall ecosystem functioning. In addition, special attention should be placed when contaminated sites are near regulated rivers, as surface water fluctuations can affect the transport of contaminants and mixing in the subsurface, either along the river corridors (Rizzo et al., 2020; Zachara et al., 2016) or in the underlying aquifer (Ziliotto et al., 2021).

7. Conclusions

In this study, we have presented a new methodology to assess the impact of surface water management on aquifers based on continuous wavelet and wavelet coherence analysis. The method takes advantage of a 7-days periodicity present in the stage of rivers impacted by hydropower production and tracks the propagation of the signal into the aquifer. The implementation of wavelet maps opens the application of the methodology for the spatio-temporal analysis of surface water - groundwater interactions and allows us to clearly delineate also in complex heterogeneous aquifers the area affected by surface water management.

Moreover, the proposed wavelet analysis shows that the 7-days periodic fluctuations in river stage have a stronger impact on the aquifer during low flow conditions, such as in winter or in dry years than in wet periods. This variability also modifies the frequency of the water exchange between river and aquifer. The consequent changes in the groundwater - surface water interactions can have chemical and biochemical implications and can cause physical variations in the transport and residence times of solutes, including contaminants.

Our study area is representative of several similar catchments in the Alpine aquifers and it allows us to test the methodology considering rivers differently affected by surface water management under similar hydrogeological and meteorological conditions. As a next step, it will be important to include also the typical uncertainty affecting the hydraulic conductivity field and how it propagates on the generated maps, as recently proposed by Merchán-Rivera, Geist, et al. (2022) in the case of groundwater flooding. Moreover, one might investigate the sensitivity of these maps considering the variability in the riverbed hydraulic conductivity and other uncertain model parameters (e.g., uncertain recharge rates, propagation of the errors in the computed river head from the hydraulic model) or the impact of the interacting 7-day fluctuations at the confluence between two rivers strongly affected by dam operations. Another possibility would be to consider longer time series to investigate the impact of reservoir management on flood events and the change of water management policies.

Overall, this manuscript shows that the effects of surface water management can significantly affect aquifers, with consequences for the water, solute and energy fluxes between surface and subsurface water. In this sense, water regulatory agencies should monitor aquifers affected by surface water management considering this increased dynamic behavior in comparison to aquifers that display a lower temporal variability. In our view, this would provide fundamental information useful to improve the management of the ecosystem's functioning.

Acknowledgments
The authors thank Gianluca Tomasi from the Geological Survey of Trento for his help providing data and in the monitoring campaigns. This research is a result of the UNMIX project (UNcertainties due to boundary conditions in predicting MIXing in groundwater), which is supported by the Deutsche Forschungsgemeinschaft (DFG) through the TUM International Graduate School for Science and Engineering (IGSSE). Additional financial support for G. Chiogna, G. Marcolini, and B. Wohlmuth was provided by DFG in the Project Hydromix (CH 981/4-1 and WO 671/16-1). B. Wohlmuth and T. Singh were funded by the DFG WO 671/11-1. M. Basilio Hazas also acknowledges the Mexican National Council for Science and Technology (CONACYT) and the Consejo Veracruzano de Investigación Científica y Desarrollo Tecnológico (COVEICYDET). Open Access funding enabled and organized by Projekt DEAL.

Data Availability Statement

Data sets for this research are available in this in-text data citation reference: Basilio Hazas et al. (2022). "Drought Conditions Enhance Groundwater Table Fluctuations caused by Hydropower Plant Management", Mendeley Data, V1, https://doi.org/10.17632/97jchhz4s8.2.

References

Agarwal, A., Maheswaran, R., Kurths, J., & Khosa, R. (2016). Wavelet spectrum and self-organizing maps-based approach for hydrologic regionalization -a case study in the Western United States. *Water Resources Management*, *30*(12), 4399–4413. https://doi.org/10.1007/s11269-016-1428-1

Agarwal, A., Maheswaran, R., Sehgal, V., Khosa, R., Sivakumar, B., & Bernhofer, C. (2016). Hydrologic regionalization using wavelet-based multiscale entropy method. *Journal of hydrology*, *538*, 22–32. https://doi.org/10.1016/j.jhydrol.2016.03.023

Autorità di bacini distrentualle delle Alpi Orientali (2010). Piano di gestione dei bacini idrografici delle alpi orientali–Bacino del fiume adige. Retrieved from http://www.alpiorientali.it/direttiva-2000-60/piano-di-gestione-acque-2010-2015/piano-approvato.html

Autorità di Bacino del Fiume Adige (2007). *Periodico trimestrale a cura dell'Autoritá Di Bacino del Fiume Adige*. Provincia Autonoma di Trento.

Bakker, M., Post, V., Langevin, C. D., Hughes, J. D., White, J. T., Starn, J. J., & Fienen, M. N. (2016). Scripting MODFLOW model development. *Using Python and FloPy: Groundwater*, *54*, 733–739. https://doi.org/10.1111/gwat.12413

Basilio Hazas, M., & Chiogna, G. (2022). Effects of highly transient boundary conditions on groundwater solute transport. *Proceedings of the 39th IAHR World Congress*. https://doi.org/10.3850/iahr-39wc252171192022763

Basilio Hazas, M., Marcolini, G., Castagna, M., Galli, M., Singh, T., Wohlmuth, B., & Chiogna, G. (2022). *Drought conditions enhance groundwater table fluctuations caused by hydropower plant management"* (pp. V2). Mendeley Data. https://doi.org/10.17632/97jchhz4s8.2

Béjar, M., Vericat, D., Batalla, R., & Gibbins, C. (2018). Variation in flow and suspended sediment transport in a montane river affected by hydropeaking and instream mining. *Geomorphology*, *310*, 69–83.

Bejarano, M. D., Jansson, R., & Nilsson, C. (2018). The effects of hydropeaking on riverine plants: A review. *Biological Reviews*, *93*(1), 658–673. https://doi.org/10.1111/brv.12362

Beretta, G. P. (2011). *Progetto per la definizione strumenti gestionali delle acque sotterranee con L'ausilio di modelli idrogeologici*. I. Provincia autonoma di trento.

Bittner, D., Engel, M., Wohlmuth, B., Labat, D., & Chiogna, G. (2021). Temporal scale-dependent sensitivity analysis for hydrological model parameters using the discrete wavelet transform and active subspaces. *Water Resources Research*, *57*(10). https://doi.org/10.1029/2020WR028511

Boutt, D. F., & Fleming, B. J. (2009). Implications of anthropogenic river stage fluctuations on mass transport in a valley fill aquifer. *Water Resources Research*, *45*(4). https://doi.org/10.1029/2007wr006526

Bruno, M. C., Maiolini, B., Carolli, M., & Silveri, L. (2009). Impact of hydropeaking on hyporheic invertebrates in an Alpine stream (Trentino, Italy). *Annales de Limnologie–International Journal of Limnology*, *45*(3), 157–170. https://doi.org/10.1051/limn/2009018

Bruno, M. C., Siviglia, A., Carolli, M., & Maiolini, B. (2013). Multiple drift responses of benthic invertebrates to interacting hydropeaking and thermopeaking waves. *Ecohydrology*, *6*(4), 511–522. https://doi.org/10.1002/eco.1275

Carolli, M., Geneletti, D., & Zolezzi, G. (2017). Assessing the impacts of water abstractions on river ecosystem services: An eco-hydraulic modelling approach. *Environmental Impact Assessment Review*, *63*, 136–146. https://doi.org/10.1016/j.eiar.2016.12.005

Casas-Mulet, R., Alfredsen, K., Hamududu, B., & Timalsina, N. P. (2015). The effects of hydropeaking on hyporheic interactions based on field experiments. *Hydrological Processes*, *29*(6), 1370–1384.

Castagna, M. (2017). Raccolta ed elaborazione di dati dinamici della parte settentrionale della valle dell'Adige.

Castagna, M., Bellin, A., & Chiogna, G. (2015). Uncertainty estimation and evaluation of shallow aquifers' exploitability: The case study of the Adige Valley aquifer (Italy). *Water*, *7*(7), 3367–3395. https://doi.org/10.3390/w7073367

Chen, D., Gao, G., Xu, C.-Y., Guo, J., & Ren, G. (2005). Comparison of the thornthwaite method and pan data with the standard Penman-Monteith estimates of reference evapotranspiration in China. *Climate Research*, *28*(2), 123–132. https://doi.org/10.3354/cr028123

Chen, K., Chen, X., Song, X., Briggs, M. A., Jiang, P., Shuai, P., et al. (2022). Using ensemble data assimilation to estimate transient hydrologic exchange flow under highly dynamic flow conditions. *Water Resources Research*, *58*, e2021WR030735. https://doi.org/10.1029/2021WR030735

Chiogna, G., Majone, B., Paoli, K. C., Diamantini, E., Stella, E., Mallucci, S., et al. (2016). A review of hydrological and chemical stressors in the Adige catchment and its ecological status. *Science of the Total Environment*, *540*, 429–443. https://doi.org/10.1016/j.scitotenv.2015.06.149

Chiogna, G., Marcolini, G., Liu, W., Pérez Ciria, T., & Tuo, Y. (2018). Coupling hydrological modeling and support vector regression to model hydropeaking in alpine catchments. *Science of the Total Environment*, *633*, 220–229. https://doi.org/10.1016/j.scitotenv.2018.03.162

Chiogna, G., Skrobanek, P., Narany, T. S., Ludwig, R., & Stumpp, C. (2018b). Effects of the 2017 drought on isotopic and geochemical gradients in the Adige catchment, Italy. *Science of the Total Environment*, *645*, 924–936. https://doi.org/10.1016/j.scitotenv.2018.07.176

Choi, B., & Choi, S.-U. (2018). Impacts of hydropeaking and thermopeaking on the downstream habitat in the Dal River, Korea. *Ecological Informatics*, *43*, 1–11. https://doi.org/10.1016/j.ecoinf.2017.10.016

Derx, J., Blaschke, A., & Blöschl, G. (2010). Three-dimensional flow patterns at the river–aquifer interface—A case study at the Danube. *Advances in Water Resources*, *33*(11), 1375–1387. https://doi.org/10.1016/j.advwatres.2010.04.013

Dountcheva, I., Sanz, D., Cassiraga, E., Galabov, V., & Gómez-Alday, J. J. (2020). Identifying non-stationary and long-term river–aquifer interactions as a response to large climatic patterns and anthropogenic pressures using wavelet analysis (Mancha Oriental Aquifer, Spain). *Hydrological Processes*, *34*(25), 5134–5145. https://doi.org/10.1002/hyp.13934

European Commission. (2016). Common implementation strategy for the water framework directive (2000/60/EC): Guidance document No. 31. In *Ecological flows in the implementation of the water framework directive: Technical report -2015 – 86*. Luxembourg: Publications Office.

Ferencz, S. B., Cardenas, M. B., & Neilson, B. T. (2019). Analysis of the effects of dam release properties and ambient groundwater flow on surface water-groundwater exchange over a 100-km-long reach. *Water Resources Research*, *55*(11), 8526–8546. https://doi.org/10.1029/2019wr025210

Fette, M., Weber, C., Peter, A., & Wehrli, B. (2007). Hydropower production and river rehabilitation: A case study on an Alpine river. *Environmental Modeling & Assessment*, *12*(4), 257–267. https://doi.org/10.1007/s10666-006-9061-7

Francis, B. A., Francis, L. K., & Cardenas, M. B. (2010). Water table dynamics and groundwater–surface water interaction during filling and draining of a large fluvial island due to dam-induced river stage fluctuations. *Water Resources Research*, *46*(7). https://doi.org/10.1029/2009wr008694

Gomez-Velez, J., Wilson, J., Cardenas, M., & Harvey, J. (2017). Flow and residence times of dynamic river bank storage and sinuosity-driven hyporheic exchange. *Water Resources Research*, *53*(10), 8572–8595. https://doi.org/10.1002/2017WR021362

Graham, E. B., Stegen, J. C., Huang, M., Chen, X., & Scheibe, T. D. (2019). Subsurface biogeochemistry is a missing link between ecology and hydrology in dam-impacted river corridors. *Science of the Total Environment*, *657*, 435–445. https://doi.org/10.1016/j.scitotenv.2018.11.414

Grinsted, A., Moore, J. C., & Jevrejeva, S. (2004). Application of the cross wavelet transform and wavelet coherence to geophysical time series. *Nonlinear Processes in Geophysics*, *11*(5/6), 561–566. https://doi.org/10.5194/npg-11-561-2004

Harbaugh, A. W. (1990). A computer program for calculating subregional water budgets using results from the U.S. Geological Survey modular three-dimensional ground-water flow model. *U.S. Geological Survey Open-File Report 90–392*, *46*. https://doi.org/10.3133/ofr90392

Harbaugh, A. W. (2005). *MODFLOW-2005, the US geological Survey modular groundwater model: The groundwater flow process*. US Department of the Interior, US Geological Survey Reston.

Hauer, C., Holzapfel, P., Leitner, P., & Graf, W. (2017). Longitudinal assessment of hydropeaking impacts on various scales for an improved process understanding and the design of mitigation measures. *Science of the Total Environment*, *575*, 1503–1514. https://doi.org/10.1016/j.scitotenv.2016.10.031

Hauer, C., Holzapfel, P., Tonolla, D., Habersack, H., & Zolezzi, G. (2019). In situ measurements of fine sediment infiltration (FSI) in gravel-bed rivers with a hydropeaking flow regime. *Earth Surface Processes and Landforms*, *44*(2), 433–448. https://doi.org/10.1002/esp.4505

Hinton, M., Schiff, S., & English, M. (1997). The significance of storms for the concentration and export of dissolved organic carbon from two Precambrian Shield catchments. *Biogeochemistry*, *36*(1), 67–88. https://doi.org/10.1023/a:1005779711821

Inamdar, S. P., Christopher, S. F., & Mitchell, M. J. (2004). Export mechanisms for dissolved organic carbon and nitrate during summer storm events in a glaciated forested catchment in New York, USA. *Hydrological Processes*, *18*(14), 2651–2661. https://doi.org/10.1002/hyp.5572

Laio, F., Porporato, A., Ridolfi, L., & Rodriguez-Iturbe, I. (2001a). Plants in water-controlled ecosystems: Active role in hydrologic processes and response to water stress: II. Probabilistic soil moisture dynamics. *Advances in Water Resources*, *24*(7), 707–723. https://doi.org/10.1016/S0309-1708(01)00005-7

Li, T., & Pasternack, G. B. (2021). Revealing the diversity of hydropeaking flow regimes. *Journal of hydrology*, *598*, 126392. https://doi.org/10.1016/j.jhydrol.2021.126392

Lu, M., Tippett, M., & Lall, U. (2015). Changes in the seasonality of tornado and favorable genesis conditions in the central United States. *Geophysical Research Letters*, *42*(10), 4224–4231. https://doi.org/10.1002/2015gl063968

Majone, B., Villa, F., Deidda, R., & Bellin, A. (2016). Impact of climate change and water use policies on hydropower potential in the south-eastern Alpine region. *Science of the Total Environment*, *543*, 965–980. https://doi.org/10.1016/j.scitotenv.2015.05.009

McCallum, J. L., & Shanafield, M. (2016). Residence times of stream-groundwater exchanges due to transient stream stage fluctuations. *Water Resources Research*, *52*(3), 2059–2073. https://doi.org/10.1002/2015wr017441

Merchán-Rivera, P., Basilio Hazas, M., Marcolini, G., & Chiogna, G. (2022). Propagation of hydropeaking waves in heterogeneous aquifers: Effects on flow topology and uncertainty quantification. *GEM–International Journal on Geomathematics*, *13*(1). https://doi.org/10.1007/s13137-022-00202-9

Merchán-Rivera, P., Geist, A., Disse, M., Huang, J., & Chiogna, G. (2022). A bayesian framework to assess and create risk maps of groundwater flooding. *Journal of hydrology*, 127797. https://doi.org/10.1016/j.jhydrol.2022.127797

Merchán-Rivera, P., Wohlmuth, B., & Chiogna, G. (2021). Identifying stagnation zones and reverse flow caused by river-aquifer interaction: An approach based on polynomial chaos expansions. *Water Resources Research*, *57*(12), e2021WR029824. https://doi.org/10.1029/2021WR029824

Moeck, C., Grech-Cumbo, N., Podgorski, J., Bretzler, A., Gurdak, J. J., Berg, M., & Schirmer, M. (2020). A global-scale dataset of direct natural groundwater recharge rates: A review of variables, processes and relationships. *Science of The Total Environment*, *717*, 137042. https://doi.org/10.1016/j.scitotenv.2020.137042

Montanari, A., Bahr, J., Blöschl, G., Cai, X., Mackay, D. S., Michalak, A. M., et al. (2015). Fifty years of water resources research: Legacy and perspectives for the science of hydrology. *Water Resources Research*, *51*(9), 6797–6803. https://doi.org/10.1002/2015wr017998

Pérez Ciria, T., & Chiogna, G. (2020). Intra-catchment comparison and classification of long-term streamflow variability in the Alps using wavelet analysis. *Journal of hydrology*, *587*, 124927. https://doi.org/10.1016/j.jhydrol.2020.124927

Pérez Ciria, T., Labat, D., & Chiogna, G. (2019). Detection and interpretation of recent and historical streamflow alterations caused by river damming and hydropower production in the Adige and Inn river basins using continuous, discrete and multiresolution wavelet analysis. *Journal of hydrology*, *578*, 124021. https://doi.org/10.1016/j.jhydrol.2019.124021

Person, E. (2013). Impact of hydropeaking on fish and their habitat.

Rizzo, C. B., Song, X., De Barros, F. P., & Chen, X. (2020). Temporal flow variations interact with spatial physical heterogeneity to impact solute transport in managed river corridors. *Journal of Contaminant Hydrology*, *235*, 103713. https://doi.org/10.1016/j.jconhyd.2020.103713

Robinson, J., & Rahmat-Samii, Y. (2004). Particle swarm optimization in electromagnetics. *IEEE Transactions on Antennas and Propagation*, *52*(2), 397–407. https://doi.org/10.1109/tap.2004.823969

Rodríguez-Iturbe, I., & Porporato, A. (2007). *Ecohydrology of water-controlled ecosystems: Soil moisture and plant dynamics*. Cambridge University Press.

Sacratees, M. (2017). Estimation of evapotranspiration in Thamirabarani River Basin using remote sensing parameter. *IJSRD–International Journal for Scientific Research & Development*, *4*(12), 602–606.

Sawyer, A. H., Bayani Cardenas, M., Bomar, A., & Mackey, M. (2009). Impact of dam operations on hyporheic exchange in the riparian zone of a regulated river. *Hydrological Processes: International Journal*, *23*(15), 2129–2137. https://doi.org/10.1002/hyp.7324

Schaefli, B., Maraun, D., & Holschneider, M. (2007). What drives high flow events in the Swiss alps? Recent developments in wavelet spectral analysis and their application to hydrology. *Advances in Water Resources*, *30*(12), 2511–2525. https://doi.org/10.1016/j.advwatres.2007.06.004

Schmadel, N. M., Ward, A. S., Lowry, C. S., & Malzone, J. M. (2016). Hyporheic exchange controlled by dynamic hydrologic boundary conditions. *Geophysical Research Letters*, *43*(9), 4408–4417. https://doi.org/10.1002/2016gl068286

Schmadel, N. M., Ward, A. S., & Wondzell, S. M. (2017). Hydrologic controls on hyporheic exchange in a headwater mountain stream. *Water Resources Research*, *53*(7), 6260–6278. https://doi.org/10.1002/2017wr020576

Shuai, P., Cardenas, M. B., Knappett, P. S., Bennett, P. C., & Neilson, B. T. (2017). Denitrification in the banks of fluctuating rivers: The effects of river stage amplitude, sediment hydraulic conductivity and dispersivity, and ambient groundwater flow. *Water Resources Research*, *53*(9), 7951–7967. https://doi.org/10.1002/2017wr020610

Shuai, P., Chen, X., Song, X., Hammond, G. E., Zachara, J., Royer, P., et al. (2019). Dam operations and subsurface hydrogeology control dynamics of hydrologic exchange flows in a regulated river reach. *Water Resources Research*, *55*(4), 2593–2612. https://doi.org/10.1029/2018wr024193

Singh, S. K. (2004). Aquifer response to sinusoidal or arbitrary stage of semipervious stream. *Journal of Hydraulic Engineering*, *130*(11), 1108–1118. https://doi.org/10.1061/(asce)0733-9429(2004)130:11(1108)

Singh, T., Wu, L., Gomez-Velez, J. D., Lewandowski, J., Hannah, D. M., & Krause, S. (2019). Dynamic hyporheic zones: Exploring the role of peak flow events on bedform-induced hyporheic exchange. *Water Resources Research*, *55*(1), 218–235. https://doi.org/10.1029/2018wr022993

Song, X., Chen, X., Stegen, J., Hammond, G., Song, H. S., Dai, H., et al. (2018). Drought conditions maximize the impact of high-frequency flow variations on thermal regimes and biogeochemical function in the hyporheic zone. *Water Resources Research*, *54*(10), 7361–7382. https://doi.org/10.1029/2018wr022586

Song, X., Chen, X., Zachara, J. M., Gomez-Velez, J. D., Shuai, P., Ren, H., & Hammond, G. E. (2020). River dynamics control transit time distributions and biogeochemical reactions in a dam-regulated river corridor. *Water Resources Research*, *56*(9), e2019WR026470. https://doi.org/10.1029/2019wr026470

Tenorio-Fernandez, L., Zavala-Hidalgo, J., & Olvera-Prado, E. (2019). Seasonal variations of river and tidal flow interactions in a tropical estuarine system. *Continental Shelf Research*, *188*, 103965. https://doi.org/10.1016/j.csr.2019.103965

Toller, G. (2002). I fabbisogni di acqua irrigua nel trentino.

Torrence, C., & Compo, G. P. (1998). A practical guide to wavelet analysis. *Bulletin of the American Meteorological Society*, *79*(1), 61–78. https://doi.org/10.1175/1520-0477(1998)079<0061:apgtwa>2.0.co;2

Torrence, C., & Webster, P. J. (1999). Interdecadal changes in the ENSO–monsoon system. *Journal of Climate*, *12*, 2679–2690. https://doi.org/10.1175/1520-0442(1999)012<2679:icitem>2.0.co;2

U. S. Army Corps of Engineers (2016). HEC-RAS river analysis system user manual.

Viesi, D., Crema, L., Zanetti, A., Galgaro, A., & Scotton, P. (2016). Geoscambio nella provincia autonoma di trento.

Welch, C., Cook, P. G., Harrington, G. A., & Robinson, N. I. (2013). Propagation of solutes and pressure into aquifers following river stage rise. *Water Resources Research*, *49*(9), 5246–5259. https://doi.org/10.1002/wrcr.20408

Wright, R., Blackett, M., & Hill-Butler, C. (2015). Some observations regarding the thermal flux from Earth's erupting volcanoes for the period of 2000 to 2014. *Geophysical Research Letters*, *42*(2), 282–289. https://doi.org/10.1002/2014gl061997

Wu, L., Gomez-Velez, J. D., Krause, S., Singh, T., Wörman, A., & Lewandowski, J. (2020). Impact of flow alteration and temperature variability on hyporheic exchange. *Water Resources Research*, *56*(3), e2019WR026225. https://doi.org/10.1029/2019wr026225

Wu, L., Singh, T., Gomez-Velez, J., Nützmann, G., Wörman, A., Krause, S., & Lewandowski, J. (2018). Impact of dynamically changing discharge on hyporheic exchange processes under gaining and losing groundwater conditions. *Water Resources Research*, *54*(12), 10076–10093. https://doi.org/10.1029/2018wr023185

Yellen, B., & Boutt, D. (2015). Hydropeaking induces losses from a river reach: Observations at multiple spatial scales. *Hydrological Processes*, *29*(15), 3261–3275. https://doi.org/10.1002/hyp.10438

Zachara, J. M., Chen, X., Murray, C., & Hammond, G. (2016). River stage influences on uranium transport in a hydrologically dynamic groundwater-surface water transition zone. *Water Resources Research*, *52*(3), 1568–1590. https://doi.org/10.1002/2015wr018009

Zachara, J. M., Chen, X., Song, X., Shuai, P., Murray, C., & Resch, C. T. (2020). Kilometer-scale hydrologic exchange flows in a gravel bed river corridor and their implications to solute migration. *Water Resources Research*, *56*(2), e2019WR025258. https://doi.org/10.1029/2019wr025258

Ziliotto, F., Basilio Hazas, M., Rolle, M., & Chiogna, G. (2021). Mixing enhancement mechanisms in aquifers affected by hydropeaking: Insights from flow-through laboratory experiments. *Geophysical Research Letters*, *48*(21), e2021GL095336. https://doi.org/10.1029/2021gl095336

Zolezzi, G., Bellin, A., Bruno, M. C., Maiolini, B., & Siviglia, A. (2009). Assessing hydrological alterations at multiple temporal scales: Adige River, Italy. *Water Resources Research*, *45*. https://doi.org/10.1029/2008wr007266

Zolezzi, G., Siviglia, A., Toffolon, M., & Maiolini, B. (2011). Thermopeaking in alpine streams: Event characterization and time scales. *Ecohydrology*, *4*(4), 564–576. https://doi.org/10.1002/eco.132

References From the Supporting Information

Carle, S. F. (1999). *T-PROGS: Transition probability geostatistical software: Users manual version 2.1* (pp. 84). University of California.

Laio, F., Porporato, A., Ridolfi, L., & Rodriguez-Iturbe, I. (2001). Plants in water-controlled ecosystems: Active role in hydrologic processes and response to water stress: II. Probabilistic soil moisture dynamics. *Advances in Water Resources*, *24*(7), 707–723. https://doi.org/10.1016/S0309-1708(01)00005-7